

# Evaluation of Radiation Shielding Properties of the Polyvinyl Alcohol/Iron Oxide Polymer Composite

K. Srinivasan<sup>1,2</sup>, E. James Jabaseelan Samuel<sup>2</sup>

<sup>1</sup>Department of Oncology, M P Birla Hospital and Priyamvada Birla Cancer Research Institute, Satna, Madhya Pradesh, <sup>2</sup>Department of Physics, School of Advanced Sciences, VIT University, Vellore, Tamil Nadu, India

## Abstract

**Context:** Lead is the conventional shielding material against gamma/X-rays. It has some limitations such as toxic, high density, nonflexibility, and also bremsstrahlung production during electron interaction. It may affect the accuracy of radiotherapy outcome. **Aims:** To theoretically analyze the radiation shielding properties of flexible polyvinyl alcohol/iron oxide polymer composite with five different concentrations of magnetite over the energy range of 15 KeV–20 MeV. **Subjects and Methods:** Radiological properties were calculated based on the published literature. Attenuation coefficients of pure elements are generated with the help of WinXCOM database. **Results:** Effective atomic numbers and electron density are increased with the concentration of magnetite. On the other hand, the number of electrons per gram decreased. Mass attenuation coefficient ( $\mu/\rho$ ) and linear attenuation coefficients ( $\mu$ ) are higher in the lower energy <100 KeV, and their values decreased when the energy increased. Computed tomography numbers (CT) show the significant variation between the concentrations in <60 KeV. Half-value layer and tenth-value layers are directly proportional to the energy and indirectly proportional to the concentration of magnetite. Transmission curve, relaxation length ( $\lambda$ ), kinetic energy released in the matter, and elemental weight fraction are also calculated and the results are discussed. **Conclusions:** 0.5% of the magnetite gives superior shielding properties compared with other concentrations. It may be due to the presence of 0.3617% of Fe. Elemental weight fraction, atomic number, photon energy, and mass densities are the important parameters to understand the shielding behavior of any material.

**Keywords:** Half-value layer, mass attenuation coefficient, polymer composite, relaxation length, shielding properties

Received on: 04-05-2017

Review completed on: 09-10-2017

Accepted on: 09-10-2017

## INTRODUCTION

Radiotherapy techniques are commonly used for the treatment of cancerous tissue and nonmalignant diseases such as pterygium, thyroid eye diseases, and pigmented villonodular synovitis. During a typical treatment, normal tissue is also exposed which is near to the treatment site, and shielding materials are used to avoid such unwanted exposure.<sup>[1]</sup> Lead is one of the commonly used shielding materials due to its physical properties and availability of different forms such as powder, glass, lead-polyethylene-boron mixture, and lead-impregnated rubber.<sup>[2]</sup> Conventional shielding materials such as mercury and lead have some limitations such as their toxicity, high cost, and higher density; due to these limitations, researchers were always interested in finding new nontoxic, cost-effective, and low-density shielding materials. Several research groups have investigated a variety of materials which satisfied these requirements.<sup>[1,3,4]</sup>

For high-density radiation shielding concrete, magnetite is the most commonly used one and it is an oxide of iron which is strongly magnetic. Low-cost and high-density hematite is also an oxide of iron which is used as gamma/X-ray shielding materials.<sup>[5]</sup> Magnetite with steel and magnetite concentrate ore, cement, and water give better radiation shielding properties compared with ordinary concrete.<sup>[6,7]</sup> Polymer composite has the advantages such as better shielding against x/gamma rays when mixed with high atomic number materials. Additionally, when mixed with hydrogen rich materials, it provides effective shielding against fast neutrons. Other benefits are less weight, commercially available, and less secondary radiation

**Address for correspondence:** Mr. K. Srinivasan,  
Department of Oncology MP Birla Hospital and Priyamvada Birla  
Cancer Research Institute, Satna - 485 005, Madhya Pradesh, India.  
E-mail: srininuclear@gmail.com

### Access this article online

Quick Response Code:



Website:  
www.jmp.org.in

DOI:  
10.4103/jmp.JMP\_54\_17

This is an open access article distributed under the terms of the Creative Commons Attribution-NonCommercial-ShareAlike 3.0 License, which allows others to remix, tweak, and build upon the work non-commercially, as long as the author is credited and the new creations are licensed under the identical terms.

**For reprints contact:** reprints@medknow.com

**How to cite this article:** Srinivasan K, Samuel EJ. Evaluation of radiation shielding properties of the polyvinyl alcohol/iron oxide polymer composite. *J Med Phys* 2017;42:273-8.

compared with pure metal shielders. It has many advantages, like protective enclosure for device and humans in hospitals, shielding spacecrafts, and nuclear power plants.<sup>[1,8,9]</sup>

Metallic polymer nanocomposite has enhanced physical properties compared with its counterparts in macroscale such as thermal, mechanical, optical, and electrical properties.<sup>[10,11]</sup> Polyethylene and borated polyethylene are used as neutron shielding materials. However, when exposed to continuous radiation, their mechanical properties, thermal stability and durability turn poor.<sup>[1]</sup> In recent years, few research groups have studied the shielding properties of polymer nanocomposite materials. Among them, Shruti Nambiar *et al.* studied the radiation shielding effectiveness of polydimethylsiloxane/bismuth oxide nanocomposite. Their result suggests that 44.44 wt% of bismuth oxide and 3.73 mm thick polydimethylsiloxane/bismuth oxide nanocomposite attenuated all the scattered radiations from 60 kV X-rays.<sup>[12]</sup> Badawy *et al.* developed a nanocomposite based on the magnetite with polyvinyl alcohol (PVA). They concluded that the PVA/magnetite nanocomposite film showed enhanced radiation shielding properties. It may be due to the fact that saturation magnetization  $M_s$  is lesser than pure magnetite due to the presence of PVA and superconducting behavior at room temperature.<sup>[13]</sup>

Radiation shielding properties of many materials have been verified by several authors with the help of theoretical calculation or experiments or both, for polymers and plastics,<sup>[4,14]</sup> superconductors,<sup>[15]</sup> alcohols, phantom and human organs and tissue substitutes,<sup>[16]</sup> silicate and borate heavy metal oxide glasses,<sup>[2]</sup> poly boron,<sup>[17]</sup> building materials,<sup>[18]</sup> various ores,<sup>[5]</sup> and some alloy materials.<sup>[19]</sup> The present analysis theoretically verifies the radiation shielding effectiveness of PVA/magnetite-polymer composite with the help of relevant radiation shielding properties over the energy range of 15 keV–20 MeV and results are compared with the previously published data.

## SUBJECTS AND METHODS

Mass attenuation coefficients ( $\mu/\rho$ ) of pure elements are generated with the help of WinXCOM database.<sup>[20]</sup> According to the published literature, radiological properties such as mass attenuation coefficient ( $\mu/\rho$ ) and gamma ray transmission factor (TF),<sup>[17]</sup> computed tomography number,<sup>[21]</sup> density,<sup>[22]</sup> effective atomic number, electron density, and the number of electron per gram are calculated.<sup>[23]</sup>

### KERMA relative to air

Mass absorption coefficients ( $\mu_{en}/\rho$ ) are connected with kinetic energy released per unit mass (KERMA) described by Manohara *et al.*<sup>[24]</sup> and Mann *et al.*<sup>[25]</sup>

$$K_a = \frac{(\mu_{en}/\rho)_{\text{Com}}}{(\mu_{en}/\rho)_{\text{air}}}$$

where,  $(\mu_{en}/\rho)_{\text{com}}$  and  $(\mu_{en}/\rho)_{\text{air}}$  are the mass energy absorption coefficients of composite and air, respectively, and  $K_a$  is the KERMA relative to air.

### Relaxation length, half-value layer, and tenth-value layer

Photon mean free path is also called relaxation length. It is defined as the average distance between the two successive interactions. This can be represented by the following equation:

$$\bar{\lambda} = \frac{\int_0^{\infty} x \exp(-\mu x) dx}{\int_0^{\infty} \exp(-\mu x) dx} = \frac{1}{\mu}$$

where,

$\mu$  ( $\text{cm}^{-1}$ ) and  $x$  are the linear attenuation coefficient and absorber thickness, respectively.  $\exp$ -is the exponential (2.718).

Half-value layer (HVL) and tenth-value layer (TVL) are defined as the attenuating material thickness required reducing the intensity as 1/2 and 1/10 of its original intensity.<sup>[17]</sup> It can be expressed as,

$$\text{HVL} = \frac{0.693}{\mu}, \text{TVL} = \frac{2.3026}{\mu}$$

## RESULTS

### Uncertainties

Uncertainties are possibly related to the mass absorption coefficient ( $\mu_{en}/\rho$ ) and mass attenuation coefficients ( $\mu/\rho$ ), which is <1% for elements ( $1 < Z < 8$ ) at 0.03–0.1 MeV. And, for photon energy  $0.03 > E > 0.1$  MeV error was 5%–10%. For medium  $Z$  elements ( $11 < Z < 29$ ) 1%–2% for 0.01–0.1 MeV and 2%–3% for 1–100 MeV.<sup>[20]</sup> These errors are not going to make much difference in our results.

### Elemental weight fraction, effective atomic number, number of electrons per gram, and electron density

Our aim was to develop the nontoxic, less weight, and flexible biological shielding materials against gamma/X-rays. At higher concentration of magnetite, polymer composite may be losing their flexibility and the weight is increased. Hence, we studied only up to 0.5% of metal oxide ( $\text{Fe}_3\text{O}_4$ ) in the PVA.

For checking the reliability of our calculation, we selected the well-known compound water and calculated its radiological properties which were in good agreement with previously published data (not shown in the manuscript). Table 1 shows calculated values of elemental weight fraction, effective atomic number ( $Z_{\text{eff}}$ ), the number of electrons per gram ( $n_e$ ), and electron density ( $\rho_e$ ) for PVA/iron oxide composite with five different concentrations of magnetite.  $Z_{\text{eff}}$  and  $\rho_e$  increased with increasing concentration of magnetite, and the numbers of electrons per gram decreased. The addition of magnetite increases the percentage of Fe (iron) in the polymer composite.

### Mass attenuation coefficient ( $\mu/\rho$ ), linear attenuation coefficient ( $\mu$ ), and computed tomography numbers (Hounsfield unit)

For the validation of attenuation coefficient, we performed the calculation for water and compared with WinXCOM

database [Figure 1]. We did not observe any significant difference. Mass attenuation coefficient ( $\mu/\rho$ ) and linear attenuation coefficient ( $\mu$ ) for PVA/iron oxide polymer composite are shown in Figures 1 and 2 respectively. Both coefficients ( $[\mu/\rho]$  and  $[\mu]$ ) are dependent on the incident photon energy and chemical composition, and these decrease with increasing the photon energy. At lower energy range, ( $\mu/\rho$ ) and ( $\mu$ ) coefficients values are higher. For incident photon energies up to 100 keV, the difference in attenuation between materials is quite evident, but it slowly decreased with increasing photon energy. Computed tomography numbers (CT) were calculated over the energy range of 0.15–20 MeV [Figure 3]. Magnetite with 0.5% concentration and 15 keV gives the highest value of CT number at 11841 Hounsfield unit (HU). And also, for energies up to 60 keV CT numbers varied much with concentration. This variation was not observed in the higher energy range. Hence, chemical composition dependence was higher in lower energy.

**Half-value layer, tenth-value layer, and transmission factor**

Figures 4 and 5 show half and TVLs of the polymer composite with an incident photon energy range of 0.015–20 MeV, respectively. In the <100 keV energy range, both HVL and TVL show sufficient deviation with respect to the concentration of magnetite and in the intermediate energy range (100 keV < E < 5

MeV) no such considerable variation was observed and for incident photon energies >5 MeV to 20 MeV little deviation was observed. In the entire photon energy range (0.015–20 MeV) 0.5% of magnetite exhibited superior behaviors compared with other concentrations, i.e., less thickness was enough to attenuate the radiation intensity to the desired level. Gamma ray TF for the material (0.5% of  $\text{Fe}_3\text{O}_4$ ) was calculated for 10 cm to 100 cm thicknesses of the polymer composite as a function of incident photon energy (0.15 MeV to 20 MeV). This is shown in Figure 6a and b. Transmittance was dependent on the incident photon energy and thickness of the material. It was higher at lower thickness of the material and higher energy of the photons. TF values are higher for polymer composite with 10–50 cm compared to the 60–100 cm thickness.

**Relaxation length ( $\lambda$ ) and KERMA relative to air**

Figure 7 represents the calculated values of relaxation length of polymer composite with five different concentrations of  $\text{Fe}_3\text{O}_4$  for the incident photon energy range of 0.015–20 MeV. It linearly increased with respect to photon energy up to 0.2 MeV and also significant difference was found between the concentrations. 0.5% of magnetite has minimum values of relaxation length compared to other concentrations. KERMA relative to air values are calculated over the photon energy range of 15 keV to 20 MeV [Figure 8]. For incident photon energies above 0.2 MeV the values were almost unity for all concentrations of magnetite, and for incident photon energies <0.2 MeV significant variation was observed.

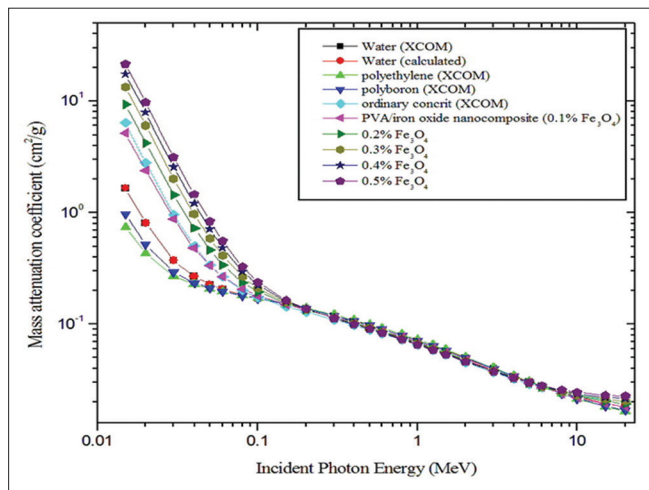


**Figure 1:** Mass attenuation coefficient for different materials plotted against incident photon energy

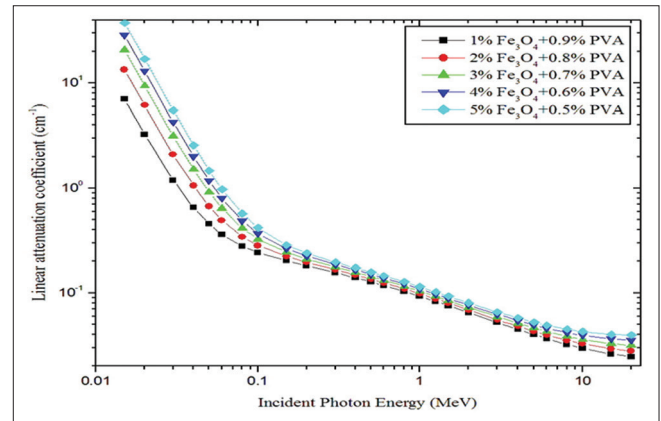


**Figure 2:** Linear attenuation coefficient for different polymer composite materials plotted against incident photon energy

**Table 1: Weight fraction of the element, number of electrons per gram, electron density, and effective atomic number of the polyvinyl alcohol/ $\text{Fe}_3\text{O}_4$  polymer composite**

Weight fraction of the compounds (Wt %)		Weight fraction of the elements (Wt %)				$N_e \times 10^{23} \text{eg}^{-1}$	$\rho_e \times 10^{24} \text{(e.cm}^{-3}\text{)}$	$Z_{\text{eff}}$
PVA	$\text{Fe}_3\text{O}_4$	WH	WC	WO	WFe			
0.9	0.1	0.082368	0.490766	0.354506	0.072360	3.238	1.997	10.958
0.8	0.2	0.073216	0.436237	0.345827	0.144720	3.196	2.15	13.391
0.7	0.3	0.064064	0.381707	0.337149	0.217080	3.154	2.293	15.221
0.6	0.4	0.054912	0.327178	0.328471	0.289440	3.112	2.441	16.738
0.5	0.5	0.045760	0.272648	0.319793	0.361799	3.071	2.589	18.060

PVA: Polyvinyl alcohol,  $N_e$ : Number of electrons per gram,  $\rho_e$ : electron density,  $Z_{\text{eff}}$ : Effective atomic number

Maximum values of KERMA relative to air were found for 30 keV for 0.5% of the magnetite which was 17.55.

## DISCUSSION

### Incident photon energy- and chemical composition-dependent shielding properties of polymer composite

Effective atomic numbers ( $Z_{\text{eff}}$ ) and electron density ( $\rho_e$ ) of the PVA/iron oxide composite increased with increasing concentration of the magnetite; it may be due to the variation in the elemental weight fraction [Table 1]. Magnetite mainly contains iron (Fe) element with an atomic number of  $Z = 26$ ; with increasing concentration of magnetite, the percentage of iron also increases in the sample.<sup>[26,27]</sup> This may be the reason behind the higher  $Z_{\text{eff}}$ ,  $\rho_e$  and lower  $n_e$  of the polymer composite with respect to increasing concentration.<sup>[28]</sup> Our calculated  $Z_{\text{eff}}$  was in good agreement with Singh *et al.* within 1.56% for PVA.<sup>[16]</sup> Another study by Manjunatha *et al.* also suggests that due to the presence of elements such as Ti, Co, Zn, As, and Cd in cancer tissues, they have higher  $Z_{\text{eff}}$ ,  $n_e$ .<sup>[21]</sup> Bone equivalence was observed at 0.2% of magnetite when compared to Jayachandran studies according to  $Z_{\text{eff}}$  values.<sup>[29]</sup> Photons are attenuated in the material via three major ways such as photoelectric absorption, Compton scatters, and pair production process.<sup>[23]</sup>

Radiological properties such as mass attenuation coefficient ( $\mu/\rho$ ), linear attenuation coefficient ( $\mu$ ), CT number (HU), KERMA relative to air, HVL, and TVL show variations between different concentrations in the lower energy range (<100 keV); it may be due to the increased photoelectric absorption.<sup>[30]</sup> Photoelectric absorption simply expressed in  $(Z/E)^3$ , where E is the energy and Z is the atomic number of the materials.<sup>[31,32]</sup> At higher concentration of magnetite, the  $Z_{\text{eff}}$  values were higher, it was around 18.060. It enables to enhance the photoelectric absorption in lower energies and considerable element composition dependence was observed. Biswas *et al.* developed and studied the shielding properties of polyboron material. They conclude that this material is used as a biological radiation shielding between the energy ranges of 0.125 MeV to 6 MeV.<sup>[17]</sup> In this regard, our calculated values of mass attenuation coefficient (PVA/iron oxide composite) was compared with their values and it was found to be superior to that of polyboron, polyethylene, and ordinary concrete [Figure 1]. Another study by Mann *et al.* studied the shielding effectiveness of polymers, plastics, and their result found that polyvinyl chloride is the best shielding material with gamma energy range of 10–110 keV.<sup>[25]</sup>

The purpose of presenting the HVL [Figure 4] and TVL [Figure 5] graphs are, choosing the appropriate thickness of the PVA/iron oxide polymer composite for shielding against particular energies of radiation (10 keV–20 MeV).<sup>[17]</sup> Relaxation length ( $\lambda$ ) is useful for the easy comparison of the shielding effectiveness of different concentrations of  $\text{Fe}_3\text{O}_4$ . Radiation shielding effectiveness of

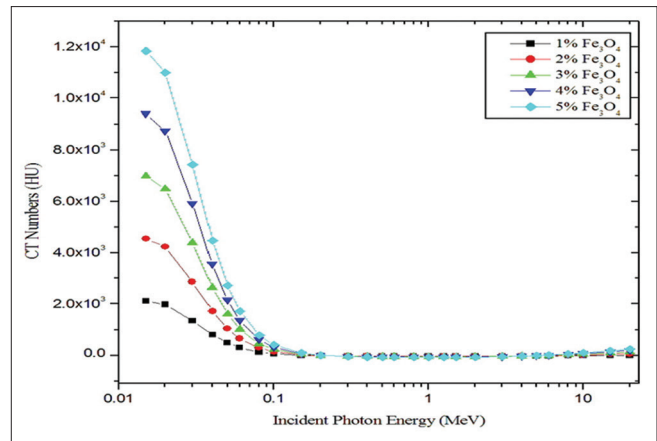


**Figure 3:** Computer tomography number for different polymer composite materials plotted against incident photon energy

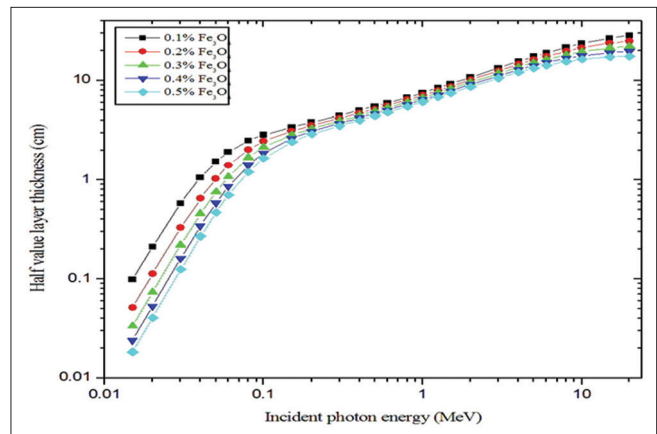


**Figure 4:** Half-value layer for different polymer composite materials plotted against incident photon energy

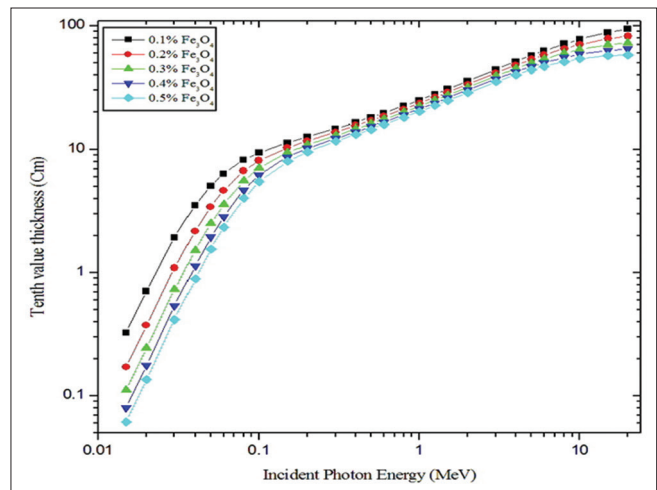


**Figure 5:** Tenth-value layer for different polymer composite materials plotted against incident photon energy

PVA/iron oxide polymer composite was varied in the following order of magnetite concentration: 0.5% > 0.4 > 0.3 > 0.2 > 0.1. For example, 0.5% of magnetite has the lower relaxation



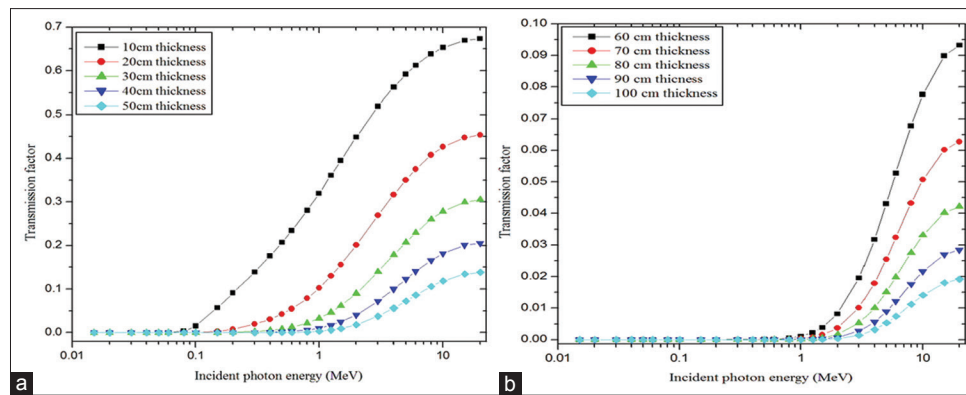


**Figure 6:** (a and b) Transmission factors for different thicknesses of polymer composite with 0.5% of magnetite plotted against incident photon energy

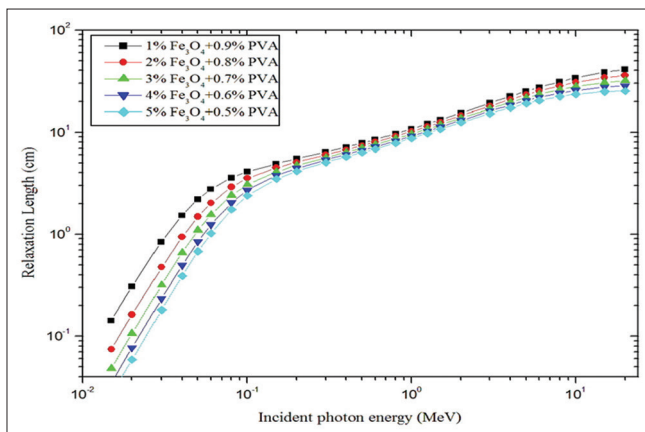


**Figure 7:** Relaxation length for concentrations of magnetite plotted against incident photon energy

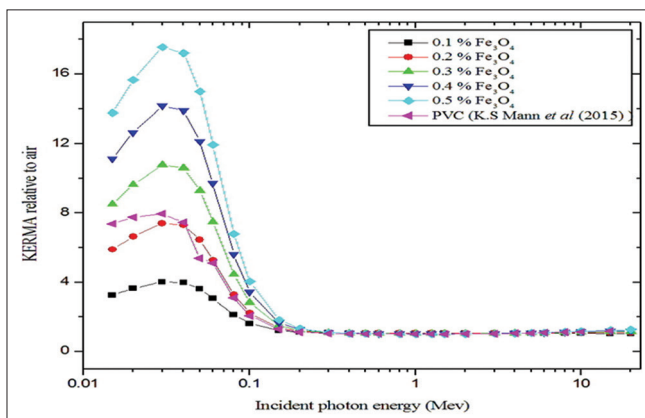


**Figure 8:** kinetic energy released per unit mass relative to air plotted against incident photon energy

length compared to 0.1% concentration. Polymer composite possessed minimum values of relaxation length at the highest concentration of magnetite [Figure 7]. Hence, we concluded that material which possessed minimum values of relaxations length offers the best shielding against gamma rays.<sup>[17]</sup> In intermediate energy range, Compton scattering is the more predominant interaction process and it is dependent on the electron density. Electron density for the polymer

composite with 0.5% of  $\text{Fe}_3\text{O}_4$  was  $2.589 \times 10^{24}$  ( $\text{e} \cdot \text{cm}^{-3}$ ).<sup>[14,30,33]</sup> Hence, in this energy range due to Compton scattering, the variation between the concentrations was not observed like photoelectric absorption region of energy; it may be due to the small variation in the electron density [Table 1].

At higher energies,  $> 1.02$  MeV small changes were observed between the concentration relative to intermediate energies. It may be due to the pair production process and it depends on the  $Z^2$  of the atomic number.<sup>[14,30]</sup> KERMA relative to air value of PVA/iron oxide composite (0.3%, 0.4%, and 0.5% of  $\text{Fe}_3\text{O}_4$ ) was superior to that previous Mann *et al.*'s study of polyvinyl chloride [Figure 8]. This simply indicates that PVA/iron oxide composite with  $\text{Fe}_3\text{O}_4$  concentration levels higher than 0.3% has better photon attenuation properties compared to polyvinyl chloride. A sharp peak located at 30 keV is the indication of higher kinetic energy released per unit mass of the composite. The presence of the higher percentage of iron makes the composite (0.5%  $\text{Fe}_3\text{O}_4$ ) to have superior photon removal capabilities compared to other lower concentration of magnetite.<sup>[34]</sup>

CT number has the direct relationship with linear attenuation coefficient ( $\mu$ ) and  $\mu$  gives the combined effect of density and materials composition ( $Z_{\text{eff}}$ ).<sup>[35]</sup> Polymer-doped  $\text{Fe}_3\text{O}_4$  is one of the contrast agents in magnetic resonance imaging.<sup>[36,37]</sup> For exploring this into computed tomography application, we studied the CT numbers of the polymer composite [Figure 3]. CT number of the conventional contrast agent iodine and soft tissue and 0.5% of the composite were compared. Results found that CT numbers were in the following order: iodine  $>$  0.5% of  $\text{Fe}_3\text{O}_4$  polymer composite  $>$  soft tissue.

## CONCLUSION

Radiation shielding properties of PVA/iron oxide polymer composite were verified with different concentrations of magnetite. Magnetite with 0.5% of concentration gives superior shielding properties according to its relative shielding parameters. At lower energy range of  $< 100$  keV, element composition dependence was more compared with other intermediate and higher energy level and it may be due to atomic number dependence of photoelectric absorption.

Further studies are needed to know the flexibility of polymer composite with different concentration of magnetite.

### Financial support and sponsorship

Nil.

### Conflicts of interest

There are no conflicts of interest.

## REFERENCES

- Nambiar S, Yeow JT. Polymer-composite materials for radiation protection. *ACS Appl Mater Interfaces* 2012;4:5717-26.
- Singh VP, Badiger NM, Kaewkhao J. Radiation shielding competence of silicate and borate heavy metal oxide glasses: Comparative study. *J Non Cryst Solids* 2014;404:167-73.
- Mann KS, Sidhu GS. Verification of some low-Z silicates as gamma-ray shielding materials. *Ann Nucl Energy* 2012;40:241-52.
- Mann KS, Rani A, Heer MA. Shielding behaviors of some polymer and plastic materials for gamma-rays. *Radiat Phys Chem* 2015;106:247-54.
- Oto B, Yıldız N, Akdemir F, Kavaz E. Investigation of gamma radiation shielding properties of various ores. *Prog Nucl Energy* 2015;85:391-403.
- Bashter II, El-Sayed Abdo A, Samir Abdel-Azim M. Magnetite ores with steel or basalt for concrete radiation shielding. *Jpn J Appl Phys* 1997;36:b92-6.
- Creutz E, Downes K. Magnetite concrete for radiation shielding. *J Appl Phys* 1949;20:1236.
- Harrison C, Weaver S, Bertelsen C, Burgett E, Hertel N, Grulke E. Polyethylene/Boron nitride composites for space radiation shielding. *J Appl Polym Sci* 2008;109:2529-38.
- Nicolais L, Carotenuto G. *Metal-Polymer Nanocomposites*. 1<sup>st</sup> ed. Vol. 1. Hoboken, New Jersey: John Wiley & Sons, Inc.; 2005.
- Harish V, Nagaiah N, Niranjana Prabhu T, Varughese KT. Preparation and characterization of lead monoxide filled unsaturated polyester based polymer composites for gamma radiation shielding applications. *J Appl Polym Sci* 2009;112:1503-8.
- Nambiar H, Yeow JT. Lead oxides filled isophthalic resin polymer composites for gamma radiation shielding applications. *Indian J Pure Ap Phy* 2012;50:847-50.
- Nambiar S, Osei EK, Yeow JT. Polymer nanocomposite-based shielding against diagnostic X-rays. *J Appl Polym Sci* 2013;127:4939-46.
- Badawy SM, Abd El-Latif AA. Synthesis and characterizations of magnetite nanocomposite films for radiation shielding. *Polym Compos* 2017;38: 974-80.
- Kucuk N, Cakir M, Isitman NA. Mass attenuation coefficients, effective atomic numbers and effective electron densities for some polymers. *Radiat Prot Dosimetry* 2013;153:127-34.
- Singh VP, Medhat ME, Badiger NM, Rahman AZ. Radiation shielding effectiveness of newly developed superconductors. *Radiat Phys Chem* 2015;106:175-83.
- Singh VP, Badiger NM. Study of effective atomic numbers and electron densities, kerma of alcohols, phantom and human organs, and tissues substitutes. *Nucl Technol Radiat Prot* 2013;28:137-45.
- Biswas R, Sahadath H, Mollah AS, Huq F. Calculation of gamma-ray attenuation parameters for locally developed shielding material: Polyboron *J Radiat Res Appl Sci* 2016;9:26-34.
- Mann KS, Kaur B, Sidhu GS, Kumar A. Investigations of some building materials for g-rays shielding effectiveness. *Radiat Phys Chem* 2013;87:16-25.
- Singh VP, Badiger NM. Gamma ray and neutron shielding properties of some alloy materials. *Ann Nucl Energy* 2014;64:301-10.
- Hubbell JH, Seltzer SM. *Tables of X-ray Mass Attenuation Coefficients and Mass Energy-Absorption Coefficients 1 keV to 20 MeV for Elements Z $\frac{1}{4}$  1 to 92 and 48 Additional Substances of Dosimetric Interest*. NISTIR-5632. Gaithersburg: National Institute of Standards and Technology; 1995.
- Manjunatha HC. Comparison of effective atomic numbers of the cancerous and normal kidney tissue. *Radiat Prot Environ* 2015;38:83-9.
- Ranjbar H, Shamsaei M, Ghasemi MR. Investigation of the dose enhancement factor of high intensity low mono-energetic X-ray radiation with labeled tissues by gold nanoparticles. *Nukleonika* 2010;55:307-12.
- Faiz Khan M. *The Physics of Radiation Therapy*. 4<sup>th</sup> ed. Maryland, USA: Williams and Wilkins Publishers; 1994.
- Manohara SR, Hanagodimath SM, Gerward L. Studies on effective atomic number, electron density and kerma for some fatty acids and carbohydrates. *Phys Med Biol* 2008;53:N377-86.
- Mann KS, Korkut T. Gamma-ray buildup factors study for deep penetration in some silicates. *Ann Nucl Energy* 2013;51:81-93.
- Sukhoruchkin SI, Soroko ZN. *Atomic Mass and Nuclear Binding Energy for Fe-56 (Iron)*. of the Series Landolt-Börnstein – Group I Elementary Particles, Nuclei and Atoms. Vol. 22A. Springer: Geneva; 2009. p. 2276-8.
- Herrmann G. *Synthesis of the Heaviest Chemical Elements-Results and Perspectives*. *Angewandte Chemie* 1998;27:1417-36.
- Gagandeep SK. Effective atomic number studies in different body tissues and amino acids. *Indian J Pure Appl Phys* 2002;40:442-9.
- Jayachandran CA. Calculated effective atomic number and kerma values for tissue-equivalent and dosimetry materials. *Phys Med Biol* 1971;16:617-23.
- Singh T, Kaur P, Singh PS. A study of photon interaction parameters in some commonly used solvents. *J Radiol Prot* 2007;27:79-85.
- Kwatra D, Venugopal A, Anant S. Nanoparticles in radiation therapy: A summary of various approaches to enhance Radiosensitization in cancer. *Transl Cancer Res* 2013;2:330-42.
- Aus RJ, DeWerd LA, Pearson DW, Micka JA, Ng KH. Dependence of scatter on atomic number for x-rays from tungsten and molybdenum anodes in the mammographic energy range. *Med Phys* 1999;26:1306-11.
- Curry TS, Dowdey JE, Murry RC. *Medical Diagnostic Radiology*. Lippincott Williams & Wilkins;1990. p. 522.
- Singh VP, Badiger NM. Investigation on radiation shielding parameters of ordinary, heavy and super heavy concretes. *Nucl Technol Radiat Prot* 2014;29:149-56.
- Hoy CF, Naquib HE, Paul N. Fabrication and control of CT number through polymeric composites based on coronary plaque CT phantom applications. *J Med Imaging (Bellingham)* 2016;3:016001.
- Arsalani N, Fattahi H, Nazarpour M. Synthesis and characterization of PVP-functionalized superparamagnetic Fe<sub>3</sub>O<sub>4</sub> nanoparticles as an MRI contrast agent. *Express Polym Lett* 2010;4:329-38.
- Ohno K, Mori C, Akashi T, Yoshida S, Tago Y, Tsujii Y, *et al.* Fabrication of contrast agents for magnetic resonance imaging from polymer-brush-afforded iron oxide magnetic nanoparticles prepared by surface-initiated living radical polymerization. *Biomacromolecules* 2013;14:3453-62.